Next-generation phylogeography of the banded newts (Ommatotriton) a phylogenetic hypothesis for three ancient species with geographically restricted interspecific gene flow and deep intraspecific genetic structure

Riemsdijk, I. van; Arntzen, J.W.; Babik, W.; Bogaerts, S.; Franzen, M.; Kalaentzis, K.; ... ; Wielstra, B.M.

Next-generation phylogeography of the banded newts (*Ommatotriton*): A phylogenetic hypothesis for three ancient species with geographically restricted interspecific gene flow and deep intraspecific genetic structure

Isolde van Riemsdijk [a,b,c], Jan W. Arntzen [a,b], Wiesław Babik [d], Sergé Bogaerts [e], Michael Franzen [f], Konstantinos Kalaentzis [a,b], Spartak N. Litvinchuk [g], Kurtuluş Olgun [h], Jan Willem P.M. Wijnands [a,b], Ben Wielstra [a,b,*]

[a] *Naturalis Biodiversity Center, P.O. Box 9517, 2300 RA Leiden, the Netherlands*
[b] *Institute of Biology Leiden, Leiden University, P.O. Box 9505, 2300 RA Leiden, the Netherlands*
[c] *Institute for Evolution and Ecology, Auf der Morgenstelle 5, D-72076, Tübingen University, Tübingen, Germany*
[d] *Institute of Environmental Sciences, Jagiellonian University, ul. Gronostajowa 7, 30-387 Kraków, Poland*
[e] *Lupinelaan 25, 5582 CG Waalre, the Netherlands*
[f] *Zoologische Staatssammlung München (ZSM-SNSB), Münchhausenstraße 21, 81247 München, Germany*
[g] *Institute of Cytology, Russian Academy of Sciences, Tikhoretsky pr. 4, 194064 St. Petersburg, Russia*
[h] *Department of Biology, Faculty of Arts and Sciences, Adnan Menderes University, 09010 Aydın, Turkey*

ABSTRACT

Technological developments now make it possible to employ many markers for many individuals in a phylogeographic setting, even for taxa with large and complex genomes such as salamanders. The banded newt (genus *Ommatotriton*) from the Near East has been proposed to contain three species (*O. nesterovi*, *O. ophryticus* and *O. vittatus*) with unclear phylogenetic relationships, apparently limited interspecific gene flow and deep intraspecific geographic mtDNA structure. We use parallel tagged amplicon sequencing to obtain 177 nuclear DNA markers for 35 banded newts sampled throughout the range. We determine population structure (with Bayesian clustering and principal component analysis), interspecific gene flow (by determining the distribution of species-diagnostic alleles) and phylogenetic relationships (by maximum likelihood inference of concatenated sequence data and based on a summary-coalescent approach). We confirm that the three proposed species are genetically distinct. A sister relationship between *O. nesterovi* and *O. ophryticus* is suggested. We find evidence for introgression between *O. nesterovi* and *O. ophryticus*, but this is geographically limited. Intraspecific structuring is extensive, with the only recognized banded newt subspecies, *O. vittatus cilicensis*, representing the most distinct lineage below the species level. While mtDNA mostly mirrors the pattern observed in nuclear DNA, all banded newt species show mito-nuclear discordance as well.

1. Introduction

The vast size and complexity of the genomes of certain taxa such as amphibians hampers whole genome sequencing (Calboli et al., 2011; Gregory, 2019; Mohlhenrich and Mueller, 2016). Yet, genome reduction methods allow for many markers from across the genome to be consulted for inferring e.g. population structure and phylogenetic relationships (Davey et al., 2011). A popular method to obtain a large number of loci randomly distributed throughout the genome is restriction-site associated DNA (RAD) sequencing (Baird et al., 2008). A

downside of this technique is that the number of shared restriction sites decreases relatively rapidly with increasing genetic divergence, meaning that the number of homologous markers obtained across increasingly divergent species quickly drops off, therewith representing a considerable limitation of RAD-sequencing data for phylogenetic inference (Eaton et al., 2017; Lemmon and Lemmon, 2013).

Transcriptome sequencing ensures that a large number of markers with a known function are obtained (Ekblom and Galindo, 2011; Everett et al., 2011). However, the costs of sequencing transcriptomes for each individual in a typical phylogenetic dataset may be

prohibitive, and sufficient samples properly preserved for RNA extraction may be hard to obtain. Hence, a popular option is to first identify a set of markers from available transcriptome data, and subsequently amplify these for many individuals e.g. stored in ethanol collections (McCormack et al., 2013). If thousands of markers are targeted for a similar number of individuals, the initial investment of designing a target capture array makes sense (Andermann et al., 2020; McCartney-Melstad et al., 2016). However, if the aim is to obtain dozens to hundreds of homologous markers, primer-based amplification by multiplex PCR is an efficient and economic approach (Wielstra et al., 2014; Zieliński et al., 2014).

An amphibian case that would benefit from increased phylogenetic resolution concerns the Near Eastern banded newts, genus *Ommatotriton* (Fig. 1). Limited genetic and morphological markers (Bülbül and Kutrup, 2013; Üzüm et al., 2019; van Riemsdijk et al., 2017) suggest that this genus comprises three species: the Anatolian banded newt *O. nesterovi* (Litvinchuk et al., 2005), the Caucasian banded newt *O. ophryticus* (Berthold, 1846) and the southern banded newt *O. vittatus* (Gray, 1835). This species radiation arose in a relatively short timeframe, a relatively long time ago (c. 25 Ma; van Riemsdijk et al., 2017): conditions under which phylogeny reconstruction is notoriously difficult (Degnan and Rosenberg, 2006; Philippe et al., 2011; Whitfield and Lockhart, 2007). The phylogenetic relationships among the three banded newt species have not yet convincingly been resolved. Different datasets provide support for each of the three possible bifurcating topologies (Arntzen and Olgun, 2000; Bülbül and Kutrup, 2013; Litvinchuk et al., 2005),

while the most recent and complete phylogenetic study to date (van Riemsdijk et al., 2017) argued that the banded newt phylogeny is currently best considered an unresolved trichotomy.

Whereas the range of *O. vittatus* is allopatric from the other two species, *O. nesterovi* and *O. ophryticus* are expected to meet in northern Turkey (Fig. 1). The latter two species are known to hybridize in an introduced population in Spain (van Riemsdijk et al., 2018). There is no evidence that this happens in nature as well, but quite possibly this reflects limited sampling in the area where the natural contact zone is expected to occur (van Riemsdijk et al., 2017). Yet, two other newt genera that are co-distributed along the southern shore of the Black Sea, *Triturus* and *Lissotriton*, show geographically extensive asymmetric introgression (Nadachowska and Babik, 2009; Wielstra et al., 2017). No introgression was reported in *Ommatotriton*, but only a very limited number of DNA markers (four, including two linked mtDNA markers) has been consulted so far (van Riemsdijk et al., 2017).

Each of the three *Ommatotriton* species is characterized by deep intraspecific mtDNA structuring (van Riemsdijk et al., 2017). It is not clear to what extent the distinct mtDNA clades are mirrored in the nuclear genome. Only one of the three banded newt species, *O. vittatus*, is currently considered polytypic (Frost, 2021), with populations from coastal south-eastern Turkey recognized as *O. v. cilicensis* (Wolterstorff, 1906). Yet, mtDNA suggests that the nominotypical subspecies of *O. vittatus* is not monophyletic (van Riemsdijk et al., 2017). Furthermore, intraspecific mtDNA divergence in *O. nesterovi* is similar to that observed in *O. vittatus*, but not recognized from the point of taxonomy.
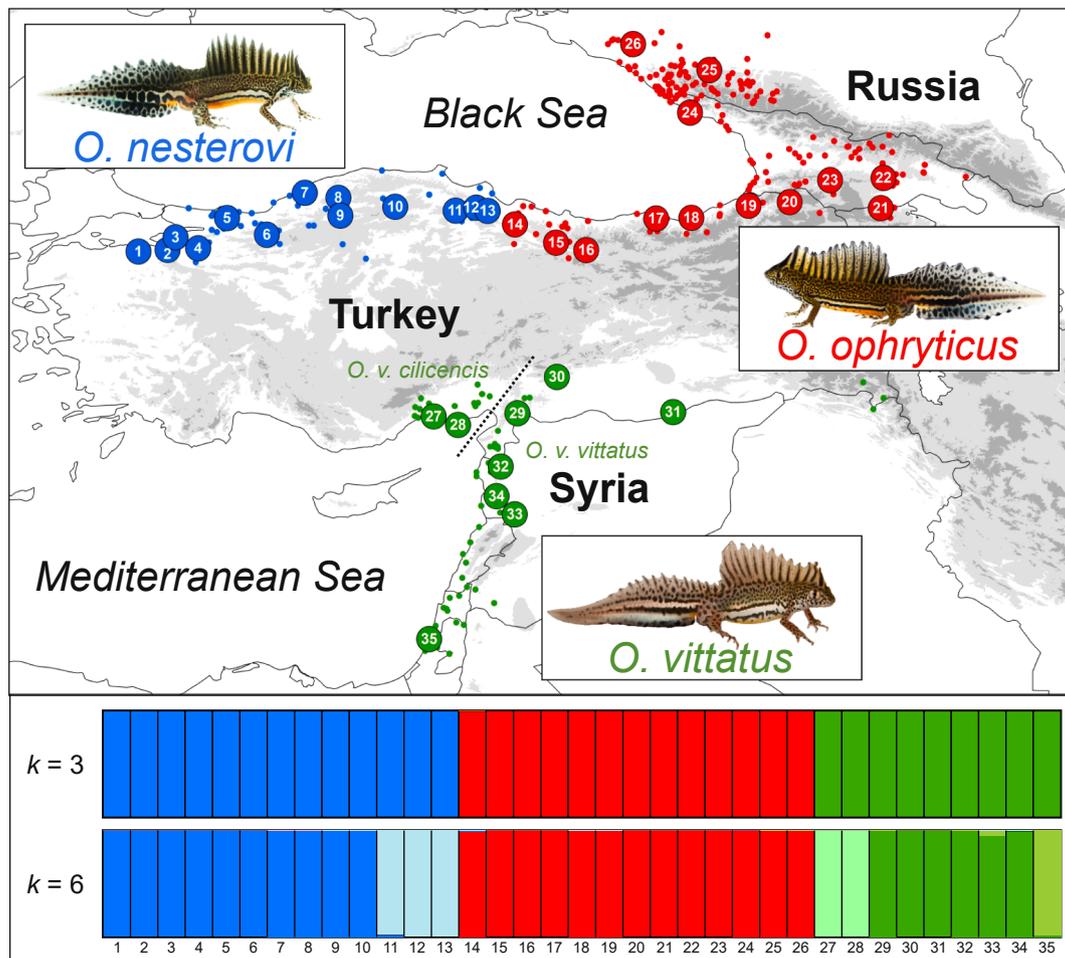
Fig. 1. Banded newt (genus *Ommatotriton*) sampling scheme and Structure plots. Dots are coloured according to species. Large dots reflect sampled sites and numbers correspond to those under the Structure plots and in Appendix 1. Small dots represent known banded newt localities (presented in Borkin et al., 2003; van Riemsdijk et al., 2017). The dotted line separates the subspecies of the only banded newt species considered to be polytypic (*O. vittatus*). (For interpretation of the references to colour in this figure legend, the reader is referred to the web version of this article.)

We design 177 transcriptome-derived nuclear markers that co-amplify across all three *Ommatotriton* species. Sequence data are obtained via multiplex PCR and Ion Torrent next-generation sequencing for 35 individuals, from the same number of localities, that span the complete banded newt distribution range (Fig. 1). With this dataset we address four questions:

1) Is there support for three banded newt species?

2) What are the phylogenetic relationships among banded newt species?

3) Is there geographically extensive, asymmetric introgression between banded newt species?

4) Is deep geographical mtDNA substructuring in banded newts mirrored in the nuclear genome?

2. Material and methods

2.1. Transcriptome assembly

We used transcriptome data of *O. nesterovi* available from Wielstra et al. (2019) and Rancilhac et al. (2021) (NCBI Sequence Read Archive Bioproject PRJNA498336, SRA accession number SAMN10659549). Data were trimmed using Trimmomatic v0.35 with default settings (Bolger et al., 2014), except for minlen, specifying the length below which a read is dropped, which we increased to 60 (from default = 36), to reduce the effect of sequencing artefacts. Trimming reduced the total number of reads from ∼ 79 million to ∼ 70 million. The transcriptome was assembled with Trinity v2.1.1, using default settings (Grabherr et al., 2011; Haas et al., 2013). The total number of 'genes' assembled was 143,433, with 175,359 transcripts (43% GC content). The N50 of all transcript contigs was 1,627, with an average contig length of 812.3, and a total number of assembled bases of 142,437,238.

2.2. Nuclear marker design

The resulting contigs were used as a database in a local BLAST search (Altschul et al., 1990), with the E-value threshold of 1E-50, against a dataset of 416 *Lissotriton* protein-coding exons screened previously to minimize the incidence of paralogs (Niedzicka et al., 2016; Stuglik and Babik, 2016). The blast results were inspected visually to identify contigs representing putative single-copy orthologs of *Lissotriton* exons. All cases where blast searches suggested multiple genes in *Ommatotriton*, i.e. when top blast hits were from multiple contigs that showed comparable similarity to the *Lissotriton* exon, were discarded. We narrowed the 325 remaining markers down to 285, by discarding those hits with a relatively low coverage or identity, because we ordered primers in batches of 95 (i.e. 3 × 95). BEDTools (Quinlan and Hall, 2010) was used to extract the sequences from the *Ommatotriton* transcriptome contigs.

2.3. Marker testing and amplification

Primers for 285 markers were designed with BatchPrimer3 (You et al., 2008), with product length set to a 160–250 bp range and a 200 bp optimum (Appendix 2). Subsequently, we selected a subset of 220 markers that consistently amplified for a single *O. nesterovi* and a single *O. ophryticus* individual. These 220 markers were amplified in 22 multiplex PCRs containing ten markers each (Appendix 3). To avoid primer dimer formation compatibility of primer combinations within individual multiplexes was tested following Wielstra et al. (2014). We used previously studied DNAs from 35 individual newts from across the entire *Ommatotriton* geographic range: 13 *O. ophryticus*, 13 *O. nesterovi*, and nine *O. vittatus* (van Riemsdijk et al., 2017; Fig. 1; Appendix 1). All PCRs were performed with the Qiagen Multiplex PCR Marker Kit in a 12.5 μL volume, using initial denaturation at 95℃ for 15 min, 35 cycles of denaturation at 95℃ for 30 s, annealing at 55℃ for one minute, extension at 72℃ for one minute, and a final extension step at 60℃ for 30 min. The 22 multiplex PCRs per individual were quantified on the QIAxcel system

and pooled equimolar.

2.4. Ion Torrent sequencing

Library preparation followed the manual of the NEBNext Fast DNA Library Prep Set for Ion Torrent kit (BioLabs Inc.), with the exception of using Ion Xpress Barcode Adapters (Life technologies). After an end repair step we ligated unique tags to each individual and conducted a dual bead-based size selection with Agencourt AMPure XP beads. The tagged 35 pools were quantified on the QIAxcel system and pooled equimolar. The molarity of this pool was measured on a 2100 Bioanalyzer using the DNA High sensitivity chip (Agilent Technologies) and the pool was diluted according to the calculated template dilution factor to target 10–30% of all positive Ion Sphere Particles. Template preparation and enrichment were carried out with the Ion One Touch 200 Template kit v2 DL (user guide revision 5.0) with the use of the Ion One Touch System. Quality control of the Ion One Touch 200 Ion Sphere Particles was conducted with the Ion Sphere Quality Control Kit using a Qubit 2.0 (Life Technologies).

IonTorrent amplicon sequencing was performed at Naturalis Biodiversity Center, on a Life Technologies Ion Torrent Personal Genome Machine (Ion PGM) sequencer (Rothberg et al., 2011), using one Ion-318-chip (Ion PGM 200 Sequencing Kit). Assembly of the sequences, identification of the alleles and recoding to genotypic format were performed with a pipeline for parallel tagged amplicon sequencing from Wielstra et al. (2014).

2.5. Bioinformatics

We obtained 220 million reads. Poor quality reads were filtered out by removing those with a length less than 100 bp and an average quality of less than Q20. Next, reads for each individual were mapped against the targeted nuclear markers using BWA v0.7.3 (Li and Durbin, 2009) and SNP/InDel calling was performed with SAMtools v0.1.18 (Li et al., 2009). A SAMtools quality score over Q60 was required for SNP/InDels to be retained. Subsequently, alleles were reconstructed by determining the combination of SNPs and InDels in the reads of marker-individual combinations. We only reconstructed alleles for marker-individual combinations that had at least 10 reads available. Alleles were required to be present in at least 25% of the reads to be called. A maximum of two alleles were allowed to be present, otherwise a marker-individual combination was considered failed. We only included markers for which alleles could be reconstructed for at least 20 individuals. We recovered 177 out of 220 markers, with a data matrix that was 85.3% complete, and continued with these 177 markers in downstream analyses.

2.6. Population structure

We used Structure 2.3.4 (Pritchard et al., 2000) to estimate for each individual the fraction of ancestry derived from each of *k* gene pools. Each haplotype was considered a different allele. We varied *k* over a 1–10 range and explored the optimal *k*-value under the Δ*k* criterion (Evanno et al., 2005) and Ln Pr(X|K) (Pritchard et al., 2000), as well as by exploring Structure plots under the entire range of *k*-values. We ran ten replicates per *k*-value, and used the admixture model in combination with the correlated allele frequency model, with 100,000 iterations after 10,000 iterations of burn-in. Data were compiled with CLUMPAK (Kopelman et al., 2015). We also conducted a principal component analysis with the package adegenet 2.1.2 in R (Jombart and Ahmed, 2011), based on individual genotypes, and replacing missing data with the mean of the total dataset.

2.7. Phylogeny

We aligned the FASTA files resulting from the bioinformatics

pipeline (Wielstra et al., 2014), containing sequence data for two alleles per individual for each marker, with MAFFT (Katoh and Standley, 2013). Alignment positions with > 80% gaps were removed with BMG (Criscuolo and Gribaldo, 2010). The alignments for all markers were concatenated with FASconCAT-Gs (Kück and Longo, 2014). A consensus sequence with polymorphic sites encoded by IUPAC codes was created for each individual using the SeqinR 3.6.1 package (Charif and Lobry, 2007) in R (R-Development-Core-Team, 2020). This resulted in a total alignment of 37,773 bp. We calculated *p*-distances within and among nuclear DNA clusters identified by Structure (see Results) using MEGA X (Kumar et al., 2018).

We conducted maximum likelihood inference with raxmlGUI v2.0.1 (Edler et al., 2021) on the concatenated dataset. We used the GTRGAMMA model of sequence evolution, treating each marker as a separate partition, and conducted 100 rapid bootstrap replicates. *Lissotriton vulgaris*, the species of which exon sequences were used in the marker design step, was used as an outgroup. We also conducted phylogenetic inference for each individual gene using the GTRGAMMA model in raxmlGUI v2.0.1. ASTRAL v.5.7.7 (Zhang et al., 2018) was used to obtain a summary-coalescent species tree based on the 177 individual gene trees, with individuals allocated to species based on the PCA and Structure analyses (see Results). To visualize mito-nuclear discordance, we re-analysed 1,444 bp of concatenated *COI* and *cytb* mitochondrial DNA sequences from van Riemsdijk et al. (2017), using MrBayes 3.2.7 (Ronquist et al., 2012), under the same settings as in van Riemsdijk et al. (2017), but including only the individuals for which Ion Torrent data were collected in the present study.

2.8. Species-diagnostic markers

To explore potential introgression between the presumably parapatric *O. nesterovi* and *O. ophryticus* (Fig. 1), we first identified the subset of markers that do not share alleles between the two species. We focussed on data in a genotypic format (i.e. our Structure input file). Identifying species-diagnostic markers that may potentially show introgression requires a partition of populations per species in two classes: 1) populations that are used to determine alleles that are diagnostic for the species involved and hence cannot show introgression; and 2) populations that are used to test for introgression and in which the presence of alleles of another species (i.e. introgression) is accepted to be possible in principle. Note that any decision here would be arbitrary, but we would argue that false negatives (i.e. an underestimation of introgression) would be preferable over false positives (i.e. an overestimation). Therefore, we tried to incorporate intraspecific structuring in the two included species (see Results), to avoid interpreting ancestral polymorphism shared between one species and only a subclade of the other species as introgression. We 1) used populations 1–11 for *O. nesterovi* and 16–26 for *O. ophryticus* to identify species-diagnostic alleles and 2) set populations 12–13 for *O. nesterovi* and 14–15 for *O. ophryticus* to potentially contain introgressed alleles (Fig. 1).

3. Results

3.1. Inter- and intraspecific structure

Structure under *k* = 3, the optimal *k* value based on the Δ*k* criterion, separates the three banded newt species (Fig. 1, *Q* scores in Appendix 1). The principal component analysis differentiates the three banded newt
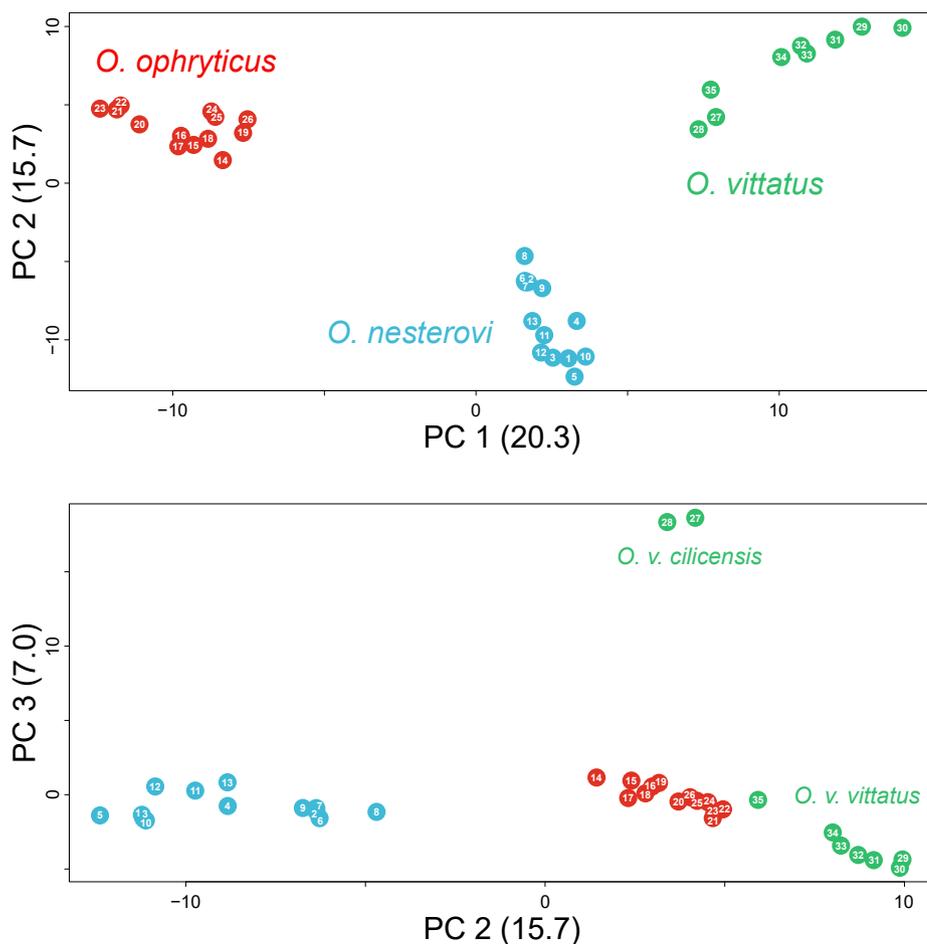

Fig. 2. Principal component analysis for banded newts (genus *Ommatotriton*). PC stands for principal component and we show plots for PC 1 versus PC 2 (above) and PC 2 versus PC 3. Values between parentheses reflect the percentage of the total variation explained by each PC. Dots are coloured according to species and numbers correspond to the sample sites in Fig. 1 and Appendix 1. (For interpretation of the references to colour in this figure legend, the reader is referred to the web version of this article.)
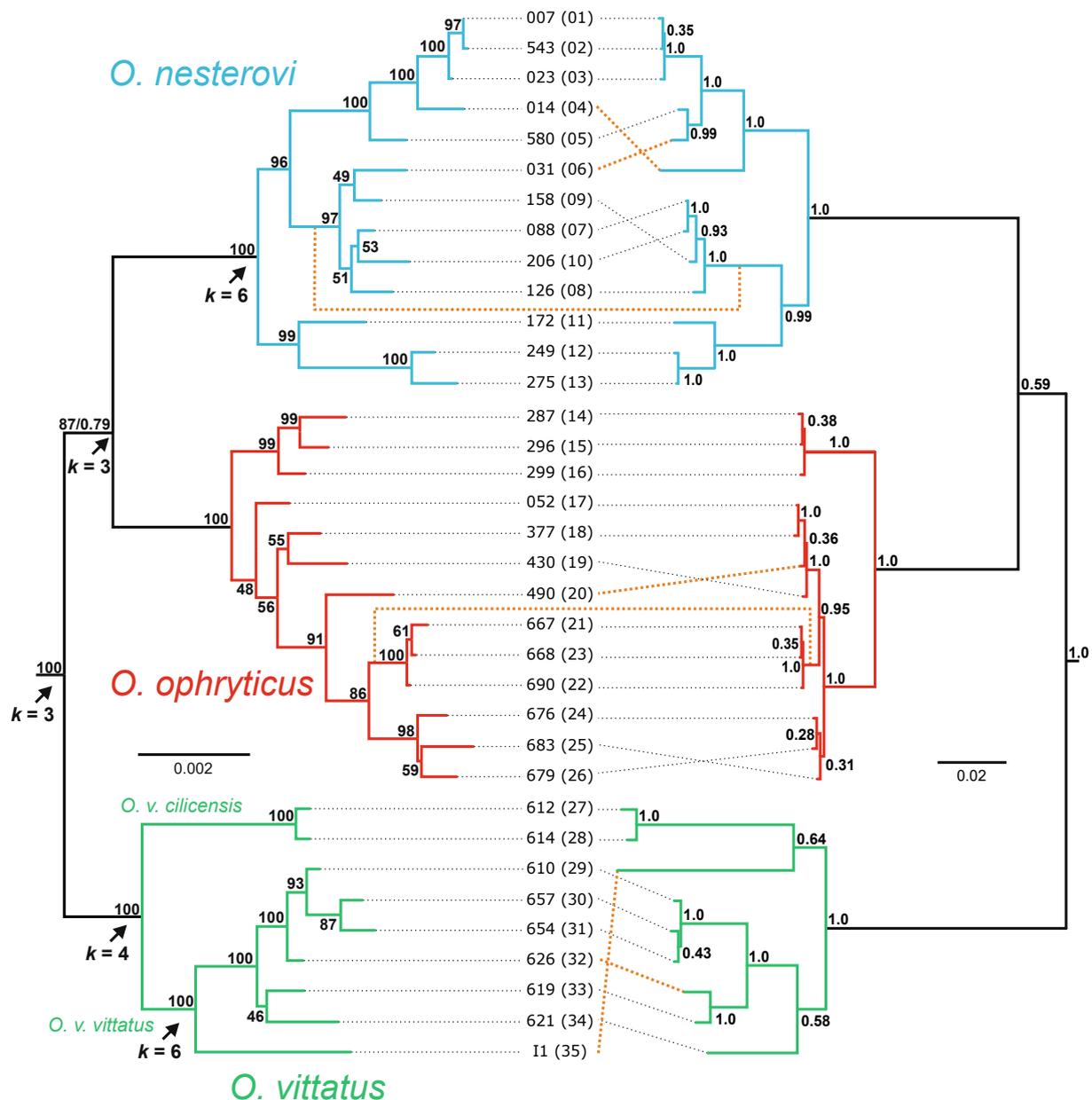
Fig. 3. Phylogenetic hypotheses for banded newts (genus *Ommatotriton*). Labels represent individuals and sample sites are in parentheses (see also Fig. 1 and Appendix 1). Black dotted lines link labels to tips and the most striking instances of mito-nuclear discordance are represented by orange interrupted lines. The maximum likelihood concatenated nuclear DNA phylogeny (left) is based on a 37,773 bp alignment of 177 nuclear DNA markers. Numbers at nodes indicate bootstrap support from 100 rapid bootstrap replicates; the one internal branch relevant for interspecific phylogenetic relationships also contains the local posterior probability received in the summary-coalescent analysis (after the slash). Clades recognized as clusters in the Structure analysis are shown with arrows (together with the relevant *k* values under which these clusters are first recognized). The Bayesian mitochondrial DNA phylogeny (right) is based on 1,444 bp of concatenated *COI* and *cytb* mitochondrial DNA sequences. Numbers at nodes indicate posterior probabilities. (For interpretation of the references to colour in this figure legend, the reader is referred to the web version of this article.)

species when plotting principal component 1 (explaining 20.3 % of the total variation) against principal component 2 (15.7%) (Fig. 2). The concatenated nuclear DNA phylogeny shows that the three *Ommatotriton* species represent reciprocally monophyletic groups (Fig. 3). The *p*-distances between species are: 0.00696 for *O. nesterovi* versus *O. ophryticus*, 0.00833 for *O. nesterovi* versus *O. vittatus* and 0.00710 for *O. ophryticus* versus *O. vittatus*.

Structure for *k* ≥ 6, which is the Ln Pr(X|K) preferred *k* value (Fig. 1, *Q* scores in Appendix 1), recognizes the two populations from the Adana delta (populations 27–28, representing *O. v. cilicensis*; see Fig. 1), the three easternmost *O. nesterovi* populations (populations 11–13), and *O. vittatus* from Israel (population 35; separated by a large area where

banded newts are known to occur but from which no populations could be sampled) as additional clusters. Exploration of Structure plots under different *k*-values (results available on Dryad) shows that for *k* ≥ 4, the Adana delta populations stand out. For the Israel population, as well as for the three easternmost *O. nesterovi* populations, this is the case under *k* ≥ 6. No clearly demarcated clusters are revealed for *k* values > 6. The concatenated nuclear DNA phylogeny shows that the three additional Structure clusters identified under *k* = 6 also represent distinct clades (although one of these is represented by only a single population, from Israel; Fig. 3). In the principal component analysis, the Adana populations stand out along principal component 3 (7.0% of total variation explained). The *p*-distances are: 0.00480 for *O. v. cilicensis* versus *O. v.*

vittatus, 0.00383 for *O. v. vittatus* from Israel versus the remainder of *O. v. vittatus* and 0.00408 for eastern versus western *O. nesterovi*.

3.2. Interspecific gene flow

No admixture between the three species is apparent from the Structure analysis (Fig. 1; Appendix 1). A closer look at the genotypic data reveals 59 markers that are species-diagnostic for *O. nesterovi* versus *O. ophryticus* (i.e. with alleles not shared between populations 1–11 and 16–26; Appendix 4). Out of these, four show potential introgression, with alleles presumed to be diagnostic for *O. nesterovi* present in *O. ophryticus* population 14 (all four markers) and population 15 (one marker). No alleles presumed to be diagnostic for *O. ophryticus* were observed in *O. nesterovi* populations.

3.3. Interspecific relationships and mito-nuclear discordance

The concatenated nuclear DNA phylogeny recovers each of the three *Ommatotriton* species as a reciprocally monophyletic group (Fig. 3). Although the concatenated nuclear DNA phylogeny does not provide unambiguous support for any of the three possible bifurcating topologies, bootstrap support for the sister species relationship between *O. nesterovi* and *O. ophryticus* at 87 is reasonably high. Yet, in the summary-coalescent analysis support for this grouping has a local posterior probability of 0.79 (the quartet score of 0.60 suggests a high degree of gene tree-species tree discordance).

Within each of the three species we observe extensive mito-nuclear discordance (Fig. 3). For *O. vittatus* both datasets suggest the presence of three main clades, but while nuclear DNA places the Israeli population (population 35) with neighbouring Middle Eastern ones (populations 29–34), mtDNA suggest (albeit with low support) a sister relationship with the allopatric subspecies *O. v. cilicensis* (populations 27–28). In *O. nesterovi* the basal split differs between the two datasets, with nuclear DNA first separating populations 1–10 vs. 11–13, and mtDNA separating populations 1–6 vs. 7–13. Whereas mitochondrial DNA finds a basal bifurcation for western (populations 14–16) and eastern *O. ophryticus* (populations 17–26), nuclear DNA does not support such a clear geographical structure; it does suggest however that the Russian and Georgian samples (populations 21–26) are nested in a paraphyletic Turkish group.

4. Discussion

4.1. Support for three distinct species

Our analyses of nuclear DNA provide firm support for the presence of three distinct species in the genus *Ommatotriton*. At the highest level of hierarchy, Structure suggests the presence of three distinct genetic clusters, corresponding to the three *Ommatotriton* species (Fig. 1). These are also the main clusters identified in the plane of the first two principal components (Fig. 2). Similarly, the concatenated nuclear DNA phylogenetic analysis recovers these three species as reciprocally monophyletic units (Fig. 3).

While salamanders are particularly vulnerable to extinction (Scheele et al., 2019), new species are regularly proposed (Frost, 2021), even in recently well-studied parts of the world (e.g. Pabijan et al., 2017; Wielstra and Arntzen, 2016). Cryptic species, distinct species that previously went unrecognized due to their morphological similarity, can be revealed through studying genetic data (Beheregaray and Caccone, 2007; Bickford et al., 2007). Once such genetically distinct species have been defined, it may be possible to find ways to tell them apart based on their phenotype (as was the case for the banded newts; Üzüm et al., 2019). Conservation first and foremost depends on a proper documentation of biodiversity and genomic tools play a crucial role in this endeavour.

4.2. A new phylogenetic hypothesis

Using two orders of magnitude more nuclear DNA markers (177 versus 2), the key node in the *Ommatotriton* phylogeny is still not unambiguously resolved. Our phylogeny based on concatenated data recovers a sister-species relationship between *O. nesterovi* and *O. ophryticus* with a reasonably high bootstrap support value of 87 (Fig. 3). However, in our summary-coalescent analysis – a theoretically sounder approach because it explicitly incorporates incomplete lineage sorting (Mirarab et al., 2014; Roch and Steel, 2015) – support for this sister-species relationship drops, with a local posterior probability of 0.79 (Fig. 3). Our study illustrates that, even with parallel tagged amplicon sequencing, it can be difficult to obtain the phylogenetic resolution required to solve phylogenies for old but rapid radiations (see e. g. Pabijan et al., 2017 for another salamander example). Alternatively, RAD-seq and target enrichment by sequence capture have been used to tackle difficult phylogenies in e.g. salamanders (Burgon et al., 2021; Rancilhac et al., 2019; Rodríguez et al., 2017; Wielstra et al., 2019). We recommend using such techniques to test the stability of our new banded newt hypothesis.

Compared to parallel tagged amplicon sequencing, the return in terms of the number of markers from RAD-seq and target enrichment by sequence capture is typically over a tenfold higher (Andermann et al., 2020; Baird et al., 2008). Yet, the increase in costs is less than double (mostly allocated to deeper sequencing and, in the case of target enrichment by sequence capture, procuring probes). Furthermore, the amount of laboratory work is reduced, because all markers are targeted during a single library preparation step, while parallel tagged amplicon sequencing requires many individual multiplex PCRs (Wielstra et al., 2014; Zieliński et al., 2014). Parallel tagged amplicon sequencing and RAD-seq use relatively little DNA compared to target enrichment by sequence capture (at least in salamander protocols; McCartney-Melstad et al., 2016; Wielstra et al., 2019). Compared to RAD-seq, parallel tagged amplicon sequencing and target enrichment by sequence capture target a highly controllable set of markers that easily cross-amplify (Andermann et al., 2020). We urge researchers to carefully weight these strengths and weaknesses when designing their study.

4.3. Little evidence for introgression

Structure suggests the absence of interspecific admixture between *O. vittatus*, with an isolated range in the Middle East (Fig. 1), and the other two banded newt species, *O. nesterovi* and *O. ophryticus*. Likewise, Structure does not suggest interspecific admixture between *O. nesterovi*, distributed along the southern shore of the Black Sea in western Asia Minor, and *O. ophryticus*, distributed along the southern Black Sea shore in eastern Asia Minor and extending into the Caucasus Mountains, even though the two are likely to meet in nature. A closer look at 59 markers presumed to be species-diagnostic for *O. nesterovi* versus *O. ophryticus* shows that for four of these markers, *O. nesterovi* alleles are observed in at least one of the two westernmost *O. ophryticus* populations (Fig. 1). This supports that introgression between *O. nesterovi* and *O. ophryticus* does occur in nature, but the geographic extent is likely to be limited.

The southern shore of the Black Sea is a suture zone, where many taxa meet in secondary contact after postglacial expansion and hybridize (Bilgin, 2011). Hybrid zones may move upon establishment, if one of the taxa involved has a competitive edge over the other (Barton and Hewitt, 1985; Buggs, 2007). Such movement would be reflected by a geographical asymmetry in introgression for many markers scattered across the genome (Currat et al., 2008; Wielstra, 2019). A genomic footprint of hybrid zone movement has been observed in the two other newt genera occurring along the southern Black Sea shore, *Triturus* (Wielstra et al., 2017) and *Lissotriton* (Nadachowska and Babik, 2009), starkly contrasting with the geographically limited reach of introgression observed in *Ommatotriton*. These patterns suggest that, while numerous hybrid zones may form in the same location after a glacial

cycle, the evolutionary history of each zone may follow a widely different course. A study of the currently undocumented contact zone is required to determine how restricted interspecific admixture is in *Ommatotriton* – the markers we provide here enable such a study.

4.4. Deep intraspecific structure and mito-nuclear discordance

Our dataset illuminates extensive intraspecific structuring within each of the *Ommatotriton* species. The only recognized *Ommatotriton* subspecies, *O. v. cilicensis* from the Adana delta (populations 27 and 28 in Fig. 1), is the first group that stands out in the Structure analysis when exploring additional clusters (i.e. *k*-values over 3). This taxon is separated from the nominotypical subspecies *O. v. vittatus* along principal component 3 in the principal component analysis (Fig. 2), and *O. v. cilicensis* and *O. v. vittatus* are reciprocally monophyletic in the concatenated nuclear DNA phylogeny (Fig. 3). The Anatolian diagonal (Ekim and Güner, 1986) poses a geographical barrier that might isolate *O. v. cilicensis* from the nominotypical subspecies. Denser sampling would be required to test for recent genetic admixture between the taxa. Our southernmost *O. vittatus* population (population 35) is also highlighted as genetically distinct (Fig. 3). The mtDNA phylogeny suggests that this population is sister to the geographically distant *O. v. cilicensis* (strong support for this sister relationship was found by van Riemsdijk et al., 2017), rather than the remainder of *O. v. vittatus* (populations 29–34) as suggested here by the concatenated nuclear DNA phylogeny. There is no indication of geographical isolation between a southern and northern population of the nominotypical subspecies and it is currently unknown if the transition between the two is abrupt or gradual; sampling between the two clusters is limited (Fig. 1) and requires further work. Note that, based on historical records (Borkin et al., 2003), there is an un-sampled, apparently isolated range section in the extreme south-eastern Turkey and northernmost Iraq (Fig. 1), but the similarly isolated, more westerly population on the boundary between Turkey and Syria turns out to be 'simply' nominotypical *O. vittatus*.

Within *O. nesterovi* we find evidence for strong population structure, with the three easternmost populations (populations 11–13) identified as distinct from the remainder (populations 1–10) by Structure (Fig. 1). The concatenated nuclear DNA phylogeny supports these two main groups as a basal bifurcation in *O. nesterovi* (Fig. 3). The genetic distance between these two groups is on par with the two subspecies recognized within *O. vittatus*. There is no obvious geographical barrier between the two genetic clusters. Our nearest populations are positioned c. 100 km apart as the crow flies and additional sampling in this region is required to determine the abruptness of the geographical transition. The concatenated nuclear DNA phylogeny suggests the reciprocal monophyly of populations 1–5 and 6–10 (Fig. 3), but this is not reflected by the Structure analysis (Fig. 1). The mtDNA phylogeny shows a quite different geographical structure, placing populations 7–10 as sister clade to populations 11–13 (Fig. 3).

Compared to the other two species, *O. ophryticus* shows a much less pronounced geographical genetic structure. The concatenated nuclear DNA phylogenetic analysis suggests a basal polytomy (Fig. 3) and Structure does not support the presence of distinct groups (Fig. 1). A basal bifurcation between western Turkey (populations 14–16) and the remainder of the range (populations 17–26), as suggested by mtDNA, is not supported by nuclear DNA. Rather, the concatenated nuclear DNA phylogenetic analysis suggests that the Russian and Georgian samples are nested in a paraphyletic Turkish group.

Strong mito-nuclear discordance, as seen in all three banded newt species, is often reported in salamanders (Pabijan et al., 2015; Recuero et al., 2014; Wielstra and Arntzen, 2020), but affects many other taxa as well (Dufresnes et al., 2020; Hogner et al., 2012; Mao et al., 2013; Zhang et al., 2019, amongst many examples). This finding underpins, once

again, that care should be taken to interpret intraspecific geographical genetic structure based on mtDNA alone.

5. Conclusions

We provide firm evidence that banded newts (genus *Ommatotriton*) contain three genetically highly distinct species: *O. nesterovi*, *O. ophryticus* and *O. vittatus*. The only recognized banded newt subspecies, *O. vittatus cilicensis*, also represents a distinct genetic lineage. Similar deep genetic divergence in *O. nesterovi* is not reflected by current taxonomy. Even with two orders of magnitude increase in the number of genetic markers, the banded phylogeny is not unambiguously resolved, with limited support for a sister relationship of *O. nesterovi* and *O. ophryticus*. While we assume that *O. nesterovi* and *O. ophryticus* meet and hybridize at a natural contact zone, we show that the geographical extent of genetic admixture between the two species must be restricted. Several cases of mito-nuclear discordance in each species convey the limitations of historical biogeographical inferences based on mtDNA alone. Our study exemplifies how the increased resolution associated with next-generation phylogeography can fine-tune and extend previous studies, based on limited marker systems.

Declaration of Competing Interest

The authors declare that they have no known competing financial interests or personal relationships that could have appeared to influence the work reported in this paper.

Appendix A. Supplementary data

Supplementary data to this article can be found online at https://doi.org/10.1016/j.ympev.2021.107361.

References

Altschul, S.F., Gish, W., Miller, W., Myers, E.W., Lipman, D.J., 1990. Basic local alignment search tool. J. Mol. Biol. 215 (3), 403–410.

Andermann, T., Torres Jiménez, M.F., Matos-Maraví, P., Batista, R., Blanco-Pastor, J.L., Gustafsson, A.L.S., Kistler, L., Liberal, I.M., Oxelman, B., Bacon, C.D., Antonelli, A., 2020. A guide to carrying out a phylogenomic target sequence capture project. Front, Genet, p. 10.

Arntzen, Olgun, K., 2000. Taxonomy of the banded newt, *Triturus vittatus*: morphological and allozyme data. Amphib.-Reptil. 21 (2), 155–168.

Baird, N.A., Etter, P.D., Atwood, T.S., Currey, M.C., Shiver, A.L., Lewis, Z.A., Selker, E.U., Cresko, W.A., Johnson, E.A., Fay, J.C., 2008. Rapid SNP discovery and genetic mapping using sequenced RAD markers. PLoS ONE 3 (10), e3376.

Barton, N.H., Hewitt, G.M., 1985. Analysis of hybrid zones. Annu. Rev. Ecol. Syst. 16 (1), 113–148.

Beheregaray, L.B., Caccone, A., 2007. Cryptic biodiversity in a changing world. J. Biol. 6 (4), 9. https://doi.org/10.1186/jbiol60.

Berthold, A., 1846. Mitteilung über das Vorkommen von Tritonen am Kaukasus. Nachrichten von der Georg-Augusts-Universität und der Königl. Gesellschaft der Wissenschaften zu Göttingen 12, 188–190.

Bickford, D., Lohman, D.J., Sodhi, N.S., Ng, P.K.L., Meier, R., Winker, K., Ingram, K.K., Das, I., 2007. Cryptic species as a window on diversity and conservation. Trends Ecol. Evol. 22 (3), 148–155.

Bilgin, R., 2011. Back to the suture: The distribution of intraspecific genetic diversity in and around Anatolia. Int. J. Mol. Sci. 12 (6), 4080–4103.

Bolger, A.M., Lohse, M., Usadel, B., 2014. Trimmomatic: a flexible trimmer for Illumina sequence data. Bioinformatics 30, 2114-2120.

Borkin, L., Litvinchuk, S., Zuiderwijk, A., 2003. Bandmolch, *Triturus vittatus* (Gray, 1835). Handbuch der Reptilien und Amphibien Europas Bd 4, 555-605.

Buggs, R.J.A., 2007. Empirical study of hybrid zone movement. Heredity 99 (3), 301–312.

Bülbül, U., Kutrup, B., 2013. Morphological and genetic variations of *Ommatotriton* in Turkey. Animal Biology 63, 297–312.

Burgon, J.D., Vences, M., Steinfartz, S., Bogaerts, S., Bonato, L., Donaire-Barroso, D., Martínez-Solano, I., Velo-Antón, G., Vieites, D.R., Mable, B.K., Elmer, K.R., 2021. Phylogenomic inference of species and subspecies diversity in the Palearctic salamander genus *Salamandra*. Mol. Phylogenet. Evol. 157, 107063. https://doi.org/10.1016/j.ympev.2020.107063.

Calboli, F.C.F., Fisher, M.C., Garner, T.W.J., Jehle, R., 2011. The need for jumpstarting amphibian genome projects. Trends Ecol. Evol. 26 (8), 378–379.

Charif, D., Lobry, J.R., 2007. SeqinR 1.0-2: a contributed package to the R project for statistical computing devoted to biological sequences retrieval and analysis. In: Structural approaches to sequence evolution. Springer, pp. 207–232.

Criscuolo, A., Gribaldo, S., 2010. BMGE (Block Mapping and Gathering with Entropy): a new software for selection of phylogenetic informative regions from multiple sequence alignments. BMC Evol. Biol. 10 (1), 210. https://doi.org/10.1186/1471-2148-10-210.

Currat, M., Ruedi, M., Petit, R.J., Excoffier, L., 2008. The hidden side of invasions: massive introgression by local genes. Evolution 62, 1908–1920.

Davey, J.W., Hohenlohe, P.A., Etter, P.D., Boone, J.Q., Catchen, J.M., Blaxter, M.L., 2011. Genome-wide genetic marker discovery and genotyping using next-generation sequencing. Nat. Rev. Genet. 12 (7), 499–510.

Degnan, J.H., Rosenberg, N.A., Wakeley, J., 2006. Discordance of species trees with their most likely gene trees. PLoS Genet. 2 (5), e68.

Dufresnes, C., Nicieza, A.G., Litvinchuk, S.N., Rodrigues, N., Jeffries, D.L., Vences, M., Perrin, N., Martínez-Solano, Í., 2020. Are glacial refugia hotspots of speciation and cytonuclear discordances? Answers from the genomic phylogeography of Spanish common frogs. Mol. Ecol. 29 (5), 986–1000.

Eaton, D.A.R., Spriggs, E.L., Park, B., Donoghue, M.J., 2017. Misconceptions on missing data in RAD-seq phylogenetics with a deep-85rtf4scale example from flowering plants. Syst. Biol. 66, 399–412.

Edler, D., Klein, J., Antonelli, A., Silvestro, D., Matschiner, M., 2021. raxmlGUI 2.0: A graphical interface and toolkit for phylogenetic analyses using RAxML. Methods Ecol. Evol. 12 (2), 373–377.

Ekblom, R., Galindo, J., 2011. Applications of next generation sequencing in molecular ecology of non-model organisms. Heredity 107 (1), 1–15.

Ekim, T., Güner, A., 1986. The Anatolian Diagonal: fact or fiction? Proceedings of the Royal Society of Edinburgh. Section B. Biological Sciences 89, 69-77.

Evanno, G., Regnaut, S., Goudet, J., 2005. Detecting the number of clusters of individuals using the software STRUCTURE: a simulation study. Mol. Ecol. 14 (8), 2611–2620.

Everett, M.V., Grau, E.D., Seeb, J.E., 2011. Short reads and nonmodel species: exploring the complexities of next-generation sequence assembly and SNP discovery in the absence of a reference genome. Mol. Ecol. Resour. 11, 93–108.

Frost, D.R., 2021. Amphibian Species of the World: an Online Reference. Version 6.1 (23 March 2021). Electronic Database accessible at http://research.amnh.org/herpetology/amphibia/index.html. American Museum of Natural History, New York, USA.

Grabherr, M.G., Haas, B.J., Yassour, M., Levin, J.Z., Thompson, D.A., Amit, I., Adiconis, X., Fan, L., Raychowdhury, R., Zeng, Q., Chen, Z., Mauceli, E., Hacohen, N., Gnirke, A., Rhind, N., di Palma, F., Birren, B.W., Nusbaum, C., Lindblad-Toh, K., Friedman, N., Regev, A., 2011. Full-length transcriptome assembly from RNA-Seq data without a reference genome. Nat. Biotechnol. 29 (7), 644–652.

Gray, 1835. A manual of British vertebrate animals. Pitt Press, Cambridge.

Gregory, T.R., 2019. Animal Genome Size Database. http://www.genomesize.com.

Haas, B.J., Papanicolaou, A., Yassour, M., Grabherr, M., Blood, P.D., Bowden, J., Couger, M.B., Eccles, D., Li, B., Lieber, M., MacManes, M.D., Ott, M., Orvis, J.,

Pochet, N., Strozzi, F., Weeks, N., Westerman, R., William, T., Dewey, C.N., Henschel, R., LeDuc, R.D., Friedman, N., Regev, A., 2013. De novo transcript sequence reconstruction from RNA-seq using the Trinity platform for reference generation and analysis. Nat. Protoc. 8 (8), 1494–1512.

Hogner, S., Laskemoen, T., Lifjeld, J.T., Porkert, J., Kleven, O., Albayrak, T., Kabasakal, B., Johnsen, A., 2012. Deep sympatric mitochondrial divergence without reproductive isolation in the common redstart *Phoenicurus phoenicurus*. Ecol. Evol. 2 (12), 2974–2988.

Jombart, T., Ahmed, I., 2011. adegenet 1.3-1: new tools for the analysis of genome-wide SNP data. Bioinformatics 27, 3070-3071.

Katoh, K., Standley, D.M., 2013. MAFFT Multiple Sequence Alignment Software Version 7: Improvements in Performance and Usability. Mol. Biol. Evol. 30, 772–780.

Kopelman, N.M., Mayzel, J., Jakobsson, M., Rosenberg, N.A., Mayrose, I., 2015. Clumpak: a program for identifying clustering modes and packaging population structure inferences across K. Mol. Ecol. Resour. 15, 1179–1191.

Kück, P., Longo, G.C., 2014. FASconCAT-G: extensive functions for multiple sequence alignment preparations concerning phylogenetic studies. Front. Zool. 11, 81.

Kumar, S., Stecher, G., Li, M., Knyaz, C., Tamura, K., 2018. MEGA X: molecular evolutionary genetics analysis across computing platforms. Mol. Biol. Evol. 35, 1547–1549.

Lemmon, E.M., Lemmon, A.R., 2013. High-throughput genomic data in systematics and phylogenetics. Annu. Rev. Ecol. Evol. Syst. 44, 99–121.

Li, H., Durbin, R., 2009. Fast and accurate short read alignment with Burrows-Wheeler transform. Bioinformatics 25 (14), 1754–1760.

Li, H., Handsaker, B., Wysoker, A., Fennell, T., Ruan, J., Homer, N., Marth, G., Abecasis, G., Durbin, R., Subgroup, G.P.D.P., 2009. The Sequence Alignment/Map format and SAMtools. Bioinformatics 25, 2078–2079.

Litvinchuk, S., Zuiderwijk, A., Borkin, L.J., Rosanov, J., 2005. Taxonomic status of *Triturus vittatus* (Amphibia: Salamandridae) in western Turkey: trunk vertebrae count, genome size and allozyme data. Amphib.-Reptil. 26, 305–323.

Mao, X., He, G., Hua, P., Jones, G., Zhang, S., Rossiter, S.J., 2013. Historical introgression and the persistence of ghost alleles in the intermediate horseshoe bat (*Rhinolophus affinis*). Mol. Ecol. 22 (4), 1035–1050.

McCartney-Melstad, E., Mount, G.G., Shaffer, H.B., 2016. Exon capture optimization in amphibians with large genomes. Mol. Ecol. Resour. 16 (5), 1084–1094.

McCormack, J.E., Hird, S.M., Zellmer, A.J., Carstens, B.C., Brumfield, R.T., 2013. Applications of next-generation sequencing to phylogeography and phylogenetics. Mol. Phylogenet. Evol. 66 (2), 526–538.

Mirarab, S., Reaz, R., Bayzid, M.S., Zimmermann, T., Swenson, M.S., Warnow, T., 2014. ASTRAL: genome-scale coalescent-based species tree estimation. Bioinformatics 30, i541–i548.

Mohlhenrich, E.R., Mueller, R.L., 2016. Genetic drift and mutational hazard in the evolution of salamander genomic gigantism. Evolution 70, 2865–2878.

Nadachowska, K., Babik, W., 2009. Divergence in the face of gene flow: the case of two newts (Amphibia: Salamandridae). Mol. Biol. Evol. 26, 829–841.

Niedzicka, M., Fijarczyk, A., Dudek, K., Stuglik, M., Babik, W., 2016. Molecular Inversion Probes for targeted resequencing in non-model organisms. Sci. Rep. 6, 24051.

Pabijan, M., Zieliński, P., Dudek, K., Chloupek, M., Sotiropoulos, K., Liana, M., Babik, W., Riddle, B., 2015. The dissection of a Pleistocene refugium: phylogeography of the smooth newt, *Lissotriton vulgaris*, in the Balkans. J. Biogeogr. 42 (4), 671–683.

Pabijan, M., Zieliński, P., Dudek, K., Stuglik, M., Babik, W., 2017. Isolation and gene flow in a speciation continuum in newts. Mol. Phylogenet. Evol. 116, 1–12.

Philippe, H., Brinkmann, H., Lavrov, D.V., Littlewood, D.T.J., Manuel, M., Wörheide, G., Baurain, D., Penny, D., 2011. Resolving difficult phylogenetic questions: why more sequences are not enough. PLoS Biol. 9 (3), e1000602.

Pritchard, J.K., Stephens, M., Donnelly, P., 2000. Inference of population structure using multilocus genotype data. Genetics 155, 945–959.

Quinlan, A.R., Hall, I.M., 2010. BEDTools: a flexible suite of utilities for comparing genomic features. Bioinformatics 26, 841–842.

R-Development-Core-Team, 2020. R: A language and environment for statistical computing. R Foundation for Statistical Computing, Vienna, Austria.

Rancilhac, L., Goudarzi, F., Gehara, M., Hemami, M.-R., Elmer, K.R., Vences, M., Steinfarz, S., 2019. Phylogeny and species delimitation of near Eastern *Neurergus* newts (Salamandridae) based on genome-wide RADseq data analysis. Mol. Phylogenet. Evol. 133, 189–197.

Rancilhac, L., Irisarri, I., Angelini, C., Arntzen, J.W., Babik, W., Bossuyt, F., Künzel, S., Lüddecke, T., Pasmans, F., Sanchez, E., Weisrock, D., Veith, M., Wielstra, B., Steinfartz, S., Hofreiter, M., Philippe, H., Vences, M., 2021. Phylotranscriptomic evidence for pervasive ancient hybridization among Old World salamanders. Mol. Phylogenet. Evol. 155, 106967. https://doi.org/10.1016/j.ympev.2020.106967.

Recuero, E., Buckley, D., García-París, M., Arntzen, J.W., Cogălniceanu, D., Martínez-Solano, Iñigo, 2014. Evolutionary history of *Ichthyosaura alpestris* (Caudata, Salamandridae) inferred from the combined analysis of nuclear and mitochondrial markers. Mol. Phylogenet. Evol. 81, 207–220.

Roch, S., Steel, M., 2015. Likelihood-based tree reconstruction on a concatenation of aligned sequence data sets can be statistically inconsistent. Theor. Popul. Biol. 100, 56–62.

Rodríguez, A., Burgon, J.D., Lyra, M., Irisarri, I., Baurain, D., Blaustein, L., Göçmen, B., Künzel, S., Mable, B.K., Nolte, A.W., Veith, M., Steinfartz, S., Elmer, K.R., Philippe, H., Vences, M., 2017. Inferring the shallow phylogeny of true salamanders (*Salamandra*) by multiple phylogenomic approaches. Mol. Phylogenet. Evol. 115, 16–26.

Ronquist, F., Teslenko, M., van der Mark, P., Ayres, D.L., Darling, A., Höhna, S., Larget, B., Liu, L., Suchard, M.A., Huelsenbeck, J.P., 2012. MrBayes 3.2: Efficient Bayesian phylogenetic inference and model choice across a large model space. Syst. Biol. 61, 539–542.

Rothberg, J.M., Hinz, W., Rearick, T.M., Schultz, J., Mileski, W., Davey, M., Leamon, J. H., Johnson, K., Milgrew, M.J., Edwards, M., Hoon, J., Simons, J.F., Marran, D., Myers, J.W., Davidson, J.F., Branting, A., Nobile, J.R., Puc, B.P., Light, D., Clark, T. A., Huber, M., Branciforte, J.T., Stoner, I.B., Cawley, S.E., Lyons, M., Fu, Y., Homer, N., Sedova, M., Miao, X., Reed, B., Sabina, J., Feierstein, E., Schorn, M., Alanjary, M., Dimalanta, E., Dressman, D., Kasinskas, R., Sokolsky, T., Fidanza, J.A., Namsaraev, E., McKernan, K.J., Williams, A., Roth, G.T., Bustillo, J., 2011. An integrated semiconductor device enabling non-optical genome sequencing. Nature 475, 348-352.

Scheele, B.C., Pasmans, F., Skerratt, L.F., Berger, L., Martel, A., Beukema, W., Acevedo, A.A., Burrowes, P.A., Carvalho, T., Catenazzi, A., De la Riva, I., Fisher, M.C., Flechas, S.V., Foster, C.N., Frías-Álvarez, P., Garner, T.W.J., Gratwicke, B., Guayasamin, J.M., Hirschfeld, M., Kolby, J.E., Kosch, T.A., La Marca, E., Lindenmayer, D.B., Lips, K.R., Longo, A.V., Maneyro, R., McDonald, C.A., Mendelson, J., Palacios-Rodriguez, P., Parra-Olea, G., Richards-Zawacki, C.L., Rödel, M.-O., Rovito, S.M., Soto-Azat, C., Toledo, L.F., Voyles, J., Weldon, C., Whitfield, S.M., Wilkinson, M., Zamudio, K.R., Canessa, S., 2019. Amphibian fungal panzootic causes catastrophic and ongoing loss of biodiversity. Science 363, 1459.

Stuglik, M.T., Babik, W., 2016. Genomic heterogeneity of historical gene flow between two species of newts inferred from transcriptome data. Ecol. Evol. 6 (13), 4513–4525.

Üzüm, N., Avcı, A., Olgun, K., Bülbül, U., Fahrbach, M., Litvinchuk, S.N., Wielstra, B., 2019. Cracking cryptic species: external characters to distinguish two recently recognized banded newt species (*Ommatotriton ophryticus* and *O. nesterovi*). Salamandra 55, 131–134.

van Riemsdijk, I., Arntzen, J.W., Bogaerts, S., Franzen, M., Litvinchuk, S.N., Olgun, K., Wielstra, B., 2017. The Near East as a cradle of biodiversity: a phylogeography of banded newts (genus *Ommatotriton*) reveals extensive inter-and intraspecific genetic differentiation. Mol. Phylogenet. Evol. 114, 73–81.

van Riemsdijk, I., van Nieuwenhuize, L., Martínez-Solano, Iñigo, Arntzen, J.W., Wielstra, B., 2018. Molecular data reveal the hybrid nature of an introduced population of banded newts (*Ommatotriton*) in Spain. Conserv. Genet. 19 (1), 249–254.

Whitfield, J.B., Lockhart, P.J., 2007. Deciphering ancient rapid radiations. Trends Ecol. Evol. 22 (5), 258–265.

Wielstra, B., 2019. Historical hybrid zone movement: more pervasive than appreciated. J. Biogeogr. 46 (7), 1300–1305.

Wielstra, B., Arntzen, J.W., 2016. Description of a new species of crested newt, previously subsumed in *Triturus ivanbureschi* (Amphibia: Caudata: Salamandridae). Zootaxa 4109, 73–80.

Wielstra, B., Arntzen, J.W., 2020. Extensive cytonuclear discordance in a crested newt from the Balkan Peninsula glacial refugium. Biol. J. Linn. Soc. 130, 578–585.

Wielstra, B., Burke, T., Butlin, R.K., Avcı, A., Üzüm, N., Bozkurt, E., Olgun, K., Arntzen, J. W., 2017. A genomic footprint of hybrid zone movement in crested newts. Evolution Letters 1, 93–101.

Wielstra, B., Duijm, E., Lagler, P., Lammers, Y., Meilink, W.R.M., Ziermann, J.M., Arntzen, J.W., 2014. Parallel tagged amplicon sequencing of transcriptome-based genetic markers for *Triturus* newts with the Ion Torrent next-generation sequencing platform. Mol. Ecol. Resour. 14, 1080–1089.

Wielstra, B., McCartney-Melstad, E., Arntzen, J.W., Butlin, R.K., Shaffer, H.B., 2019. Phylogenomics of the adaptive radiation of *Triturus* newts supports gradual ecological niche expansion towards an incrementally aquatic lifestyle. Mol. Phylogenet. Evol. 133, 120–127.

Wolterstorff, W., 1906. Über den Formenkreis des Triton (=Molge) vittatus Gray. Zool. Anz. 29, 649–654.

You, F., Huo, N., Gu, Y., Luo, M.-C., Ma, Y., Hane, D., Lazo, G., Dvorak, J., Anderson, O., 2008. BatchPrimer3: a high throughput web application for PCR and sequencing primer design. BMC Bioinformatics 9, 253.

Zhang, C., Rabiee, M., Sayyari, E., Mirarab, S., 2018. ASTRAL-III: polynomial time species tree reconstruction from partially resolved gene trees. BMC Bioinformatics 19, 153.

Zhang, D., Tang, L., Cheng, Y., Hao, Y., Xiong, Y., Song, G., Qu, Y., Rheindt, F.E., Alström, P., Jia, C., Lei, F., 2019. "Ghost introgression" as a cause of deep mitochondrial divergence in a bird species complex. Mol. Biol. Evol. 36, 2375–2386.

Zieliński, P., Stuglik, M.T., Dudek, K., Konczal, M., Babik, W., 2014. Development, validation and high throughput analysis of sequence markers in non-model species. Mol. Ecol. Resour. 14, 352–360.